

KfK 3377
Juli 1982

**Isoscalar Octupole Transition
Rates in ^{50}Ti , ^{52}Cr and ^{208}Pb
from Model-Independent
Analyses of 104 MeV
 α -Particle Scattering**

V. Corcalciuc, H. Rebel, R. Pesl, H. J. Gils
Institut für Angewandte Kernphysik

Kernforschungszentrum Karlsruhe



KERNFORSCHUNGSZENTRUM KARLSRUHE

Institut für Angewandte Kernphysik

KfK 3377

ISOSCALAR OCTUPOLE TRANSITION RATES IN
 ^{50}Ti , ^{52}Cr and ^{208}Pb FROM MODEL-INDEPENDENT ANALYSES
OF 104 MeV α -PARTICLE SCATTERING

V. Corcalciuc⁺, H. Rebel, R. Pesl, and H.J. Gils

Kernforschungszentrum Karlsruhe GmbH, Karlsruhe

⁺Central Institute of Physics, Bucharest, Romania

Als Manuskript vervielfältigt
Für diesen Bericht behalten wir uns alle Rechte vor

Kernforschungszentrum Karlsruhe GmbH
ISSN 0303-4003

ABSTRACT

Applying a recently proposed method for model-independent analyses experimental differential cross sections for 104 MeV α -particle scattering have been analyzed. Reliable values of isoscalar ($0^+ - 3_1^-$) octupole transition rates in ^{50}Ti , ^{52}Cr and ^{208}Pb are presented and compared with electromagnetic rates.

ISOSKALARE OKTUPOLE ÜBERGANGSRATEN IN ^{50}Ti , ^{52}Cr AND ^{208}Pb
AUS MODELLUNABHÄNGIGEN ANALYSEN DER 104 MeV α -TEILCHENSTREUUNG

Mit Hilfe einer kürzlich vorgeschlagenen modellunabhängigen Methode wurden die experimentellen differentiellen Wirkungsquerschnitte für 104 MeV α -Teilchenstreuung analysiert. Verlässliche Werte für die isoskalaren ($0^+ - 3_1^-$) Oktupol-Übergangsraten in ^{50}Ti , ^{52}Cr und ^{208}Pb werden angegeben und mit elektromagnetischen Raten verglichen.

1. INTRODUCTION

For a complete understanding of nuclear structure it is necessary to be able to distinguish between neutron and proton components in nuclear transitions as well as in ground state density distributions. The question of possible differences in proton and neutron transition matrix elements can be addressed by comparing the reduced electromagnetic transition strength to the corresponding reduced strength of the same transition induced by hadronic probes. Writing the neutron and proton matrix elements with multipolarity λ as

$$M_{n(p)} = \int \rho_{fi}^{n(p)}(r) r^{\lambda+2} dr \quad (1.1)$$

where

$$\rho_{fi}^{n(p)}(r) = \langle i | \sum_{j=1}^A \left(\frac{1+\tau_j^z}{2} \right) \delta(\vec{r}-\vec{r}_j) | f \rangle \quad (1.2)$$

are the neutron- and proton transition densities, respectively, the matrix element for a transition induced by an external field may be split up in

$$M = C_n M_n + C_p M_p \quad (1.3)$$

The (generally energy dependent) factors $C_{n(p)}$ characterize the sensitivity of the applied probe to neutron and proton components.

The usual collective model assumes that neutron and protons move in phase with the same amplitude ($\rho_{fi}^n/\rho_{fi}^p = N/Z$). This implies that neutron and proton matrix elements are equal (when normalized to equal particle numbers). Due to shell effects and also predicted by theoretical studies (Brown and Madsen 1978,1975, Brown and Wildenthal 1980), systematic deviations, in particular for $N \neq Z$ nuclei are expected. Several experimental studies using different methods have reported evidence of such effects (see Bernstein et al 1981). However,

in most cases the results appear to be not sufficiently conclusive and are often based more on qualitative considerations of trends than on serious discussions of the uncertainties involved. In fact, the evaluation of transition matrix elements from hadron scattering cross sections is a delicate operation and affected by several kinds of model dependence. Constraints by simple functional forms of the transition potentials (derivatives of a Saxon-Woods potential), simplified assumptions about the reaction mechanism (first order DWBA neglecting coupled channel effects) and dubious procedures relating quantities of the *interaction potential* to the *transition densities* of the target nucleus are able to produce similar effects, or mask the effects looked for and have been shown (Rebel 1976, Wagner et al 1982) to lead to wrong results occasionally. With this point of view the significance of many reported results appears to be questionable and the experimental evidence for deviations from the collective model prediction for M_n/M_p is often not convincing.

The recent progress in understanding the reaction mechanisms of intermediate energy proton scattering (Amado et al 1980) and of α -particle scattering (Friedman et al 1981) at energies of about 100 MeV has prompted the development of more reliable methods for analyzing hadron scattering in terms of transition matrix elements. The interest in α -particle scattering stems from the fact that α -particles interact equally with neutron and protons ($C_n/C_p = 1$), thus providing the pure isoscalar part of the transition probability. In this paper we report about studies of the $0^+ - 3_1^-$ octupole transitions in ^{50}Ti , ^{52}Cr and ^{208}Pb applying a recently proposed method (Rebel et al 1981) which reduces the model dependence of previous results considerably and allows serious comparisons with electromagnetic data. The analysis is based on precisely measured differential cross sections of elastic and inelastic scattering of 104 MeV α -particles (Pesi et al 1982). The cross sections cover a large angular range extending beyond the nuclear rainbow region. This feature appears to be necessary for a successful application of a quasi-model independent method.

2. DETERMINATION OF THE COUPLING POTENTIALS

Model-independent analysis of inelastic electron scattering (Dreher et al 1974) have shown that the usual parametrizations of the charge transition densities by a vibrational model or Tassie-model form factor provide good descriptions of the overall shapes, in particular in the surface region, but need clearly some refinements when looking for more detailed effects. Similarly, when determining the non-diagonal part of the α -particle-nucleus interaction potential (inducing inelastic excitation) it may be quite dangerous to constrain the shapes simply by derivatives of the diagonal potential. In order to reduce this type of model dependence we apply a recently proposed method (Rebel et al 1981) using a more flexible parametrization of the real part $v_L(r_\alpha)$ of the coupling potentials (only the detailed shape of the real part is of interest for the further discussion). The method consists of adding to a conventional form (say, the familiar derivative of a Woods-Saxon) an extra potential given by Fourier-Bessel series

$$v_L(r_\alpha) = \beta_L^{(\text{pot})} (v_{\text{coupl}}^0(r_\alpha) + \sum_{n=1}^N b_n j_1(q_n r_\alpha)). \quad (2.1)$$

The quantities j_1 are spherical Bessel functions, $q_n = n\pi/R_{\text{cut}}$ and R_{cut} is a suitably chosen cut-off radius beyond which the extra potential vanishes.

After fixing the $\beta_L^{(\text{pot})} v_{\text{coupl}}^0$ term by a first guess or a shape resulting from a best-fit with $b_n \equiv 0$, the correction coefficients b_n are determined by a least-squares fit to the data. Within the framework of the Fourier-Bessel procedure the mean-square uncertainty of $v_L(r_\alpha)$ at the distance r_α is given by

$$[\delta v_L(r_\alpha)]^2 = \sum_{m,n} \langle \delta b_m \delta b_n \rangle_{\text{av}} j_1(q_m r_\alpha) j_1(q_n r_\alpha). \quad (2.2)$$

with $\langle \delta b_m \delta b_n \rangle$ being the correlation matrix between the coefficients b_n . The residual model dependence is due to the

specific choice of the cut-off radius R_{cut} . In course of the analysis N and R_{cut} are varied.

In view of the simplifications in DWBA and in order to avoid effects due to neglect of multiple excitation, the present results are based on coupled channels calculations. Thereby we generally fit elastic and inelastic scattering simultaneously.

The real diagonal part V_{diag} has been recently studied in extensive elastic scattering analyses using model-independent techniques (Friedman et al 1981, Gils et al 1980). In particular, it has been shown that the radial shape is very well approximated by a squared Saxon-Woods form (SW^2) with parameter values which prove to be fairly well determined by the elastic scattering. Small readjustments due to coupling to the excited states have been taken into account by results of coupled channels calculations on the basis of the usual vibrational model. Therefore, for the sake of simplicity the shape of $V_{\text{diag}}(r_\alpha)$ has not been varied simultaneously with the b_n coefficients of $v_L(r_\alpha)$. Only the imaginary part has been readjusted when fitting the cross sections. Complex coupling is taken into account via the deformation $B_L^{(\text{pot})}$ of the imaginary part. Coulomb excitation is included by a deformed Coulomb potential. All calculations used a modified version of the coupled channels code ECIS (Schweimer and Raynal 1973).

Table 1 presents the parameters of the real potentials, taken either from the analysis of elastic scattering only - or from a coupled channel analysis on the basis of the usual vibrational model. Also shown are parameters of V_{trans} , the first derivative of which serves as a first guess to the FB coupling potential. We note that V_{trans} and V_{diag} have independent geometries and that the factorization of the transition potential by eq. (2.1) is only a reminder to the standard procedure. In course of the calculations it turned out that a SW shape of $V_{\text{trans}}(L=3)$ proves to be a better first guess

potential than a SW^2 shape (as simultaneously used for V_{diag}). This finding is in contrast to results when analyzing $0^+ - 2_1^+$ quadrupole transitions (Rebel et al. 1981).

Figs. 1-3 display experimental and calculated cross sections (the insets give additional information concerning the imaginary part of the potential) and Fig. 4 compares the obtained Fourier-Bessel potentials with the best-fit derivative shapes corresponding to the V_{trans} parameters quoted in Table 1. The values of R_{cut} and N have been increased up to convergence of χ^2/F and of the errors of the integral quantities (radial moments). The error bands of the potentials result from averaging several single fits with different choices of the cut-off radius R_{cut} and of the number of Fourier-Bessel terms. This procedure is expected to remove the remaining model dependence. It is interesting to see how well the derivative form approximates the resulting Fourier-Bessel potentials in the surface region. In order to preserve general requirements for the transition densities the extreme inner parts is parametrized by a polynomial with zero value at $r = 0$. This additional constraint obscures somewhat the fact that the region $r \lesssim 2$ fm is completely "black" for 104 MeV α -particle scattering. On the other side, the details and deviations from the derivative form appear to be significant for $r \geq 2$ fm. In ^{208}Pb e.g. the shape of $v_3(r_\alpha)$ resembles conspicuously the charge transition density (Fig. 5) as found by theoretical (Speth 1976, Theis and Werner 1973) and inelastic electron scattering studies (Rothaas et al 1974).

Table 1 Parameters of the real potentials used in the analysis

	V_0 [MeV]	R_V [fm]	a_V [fm]	$B_3^{(pot)}$	χ^2/F			Shape and Procedure
					Tot	0^+	3^-	
^{50}Ti	V_{Diag}	147.2			-	1.8	-	SW^2 elast.
	V_{Diag}	122.2	4.595	0.789	0.132	4.0	3.9 4.1	SW CC
	V_{Diag}	146.3	5.214	1.183	0.122	3.2	2.0 4.8	SW^2 CC
	V_{Diag}	148.9	5.166	1.196	-	1.9	- -	SW^2 +
	V_{Diag}	83.4	4.948	0.757	0.133	-	1.7 2.2	SW-Deriv.
V_{trans}	N=10-13, $R_{\text{cut}}=11-13$			0.133	1.7	1.7 1.8	SW-Deriv. +FB	
^{52}Cr	V_{Diag}	156.9	5.102	1.228	-	-	1.7 -	SW^2 elast.
	V_{Diag}	130.5	4.476	0.797	0.118	4.7	3.8 5.7	SW CC
	V_{Diag}	155.9	5.119	1.192	0.109	4.6	2.7 6.7	SW^2 CC
	V_{Diag}	165.4	4.997	1.264	-	2.5	- -	SW^2
	V_{Diag}	83.3	5.490	0.564	0.091	-	1.6 3.6	SW-Deriv.
V_{trans}	N=10-13, $R_{\text{cut}}=11-13$			0.091	1.2	1.4 0.9	SW-Deriv. + FB	
^{208}Pb	V_{Diag}	171.5	7.938	1.298	-	4.2	-	SW^2 elast.
	V_{Diag}	119.1	7.861	0.687	0.092	7.8	7.4 8.3	SW CC
	V_{Diag}	154.2	8.186	1.206	0.082	5.8	6.7 9.6	SW^2 CC
	V_{Diag}	166.3	7.976	1.308	-	4.1	- -	SW^2
	V_{Diag}	68.2	8.343	0.819	0.086	-	4.3 3.8	SW-Deriv.
V_{trans}	N=10-13, $R_{\text{cut}}=11-14$			0.086	4.1	4.3 3.8	SW-Deriv. + FB	

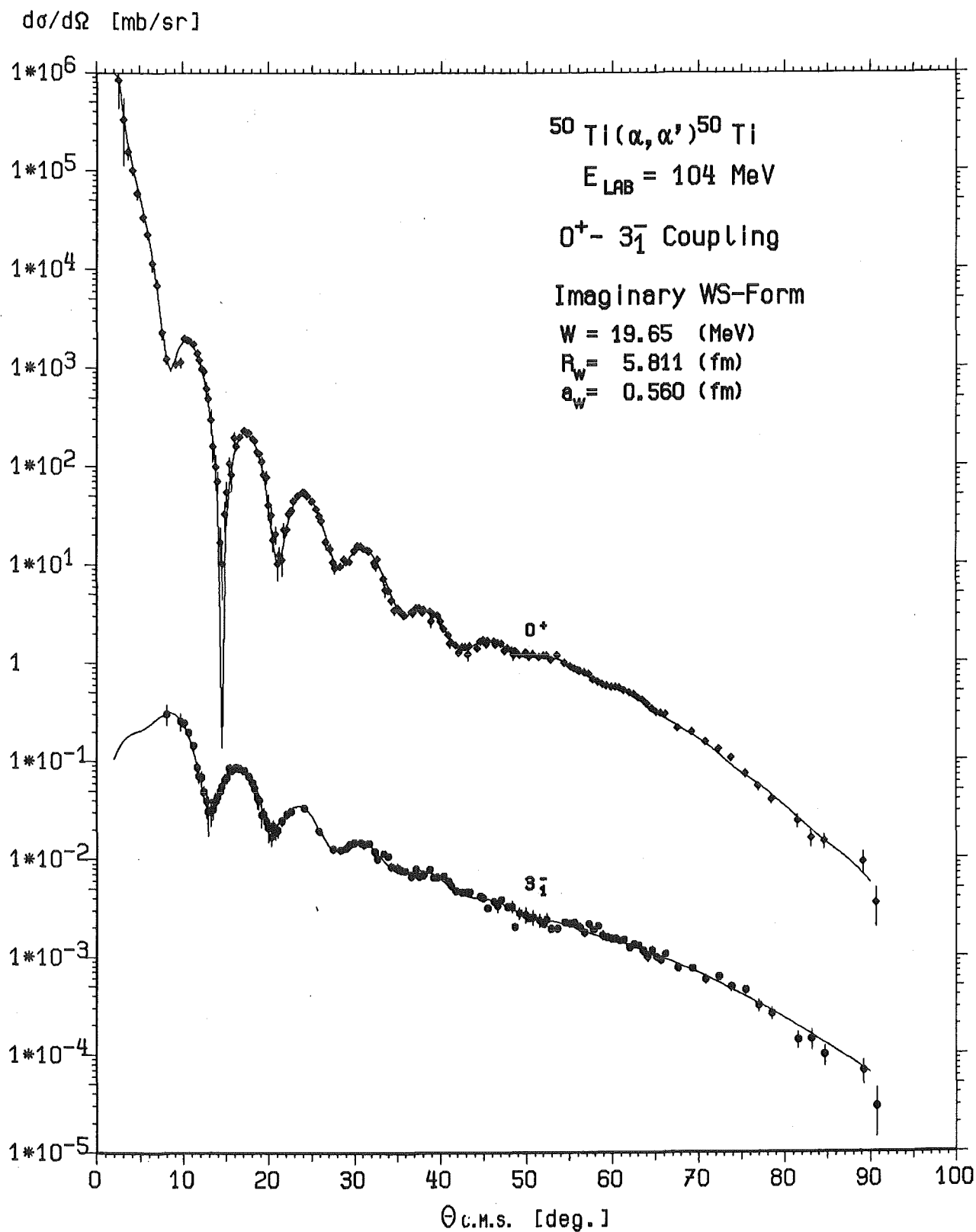


Fig. 1 Elastic and inelastic scattering of 104 MeV α -particles by ^{50}Ti : experimental cross sections and results of coupled channel calculations.

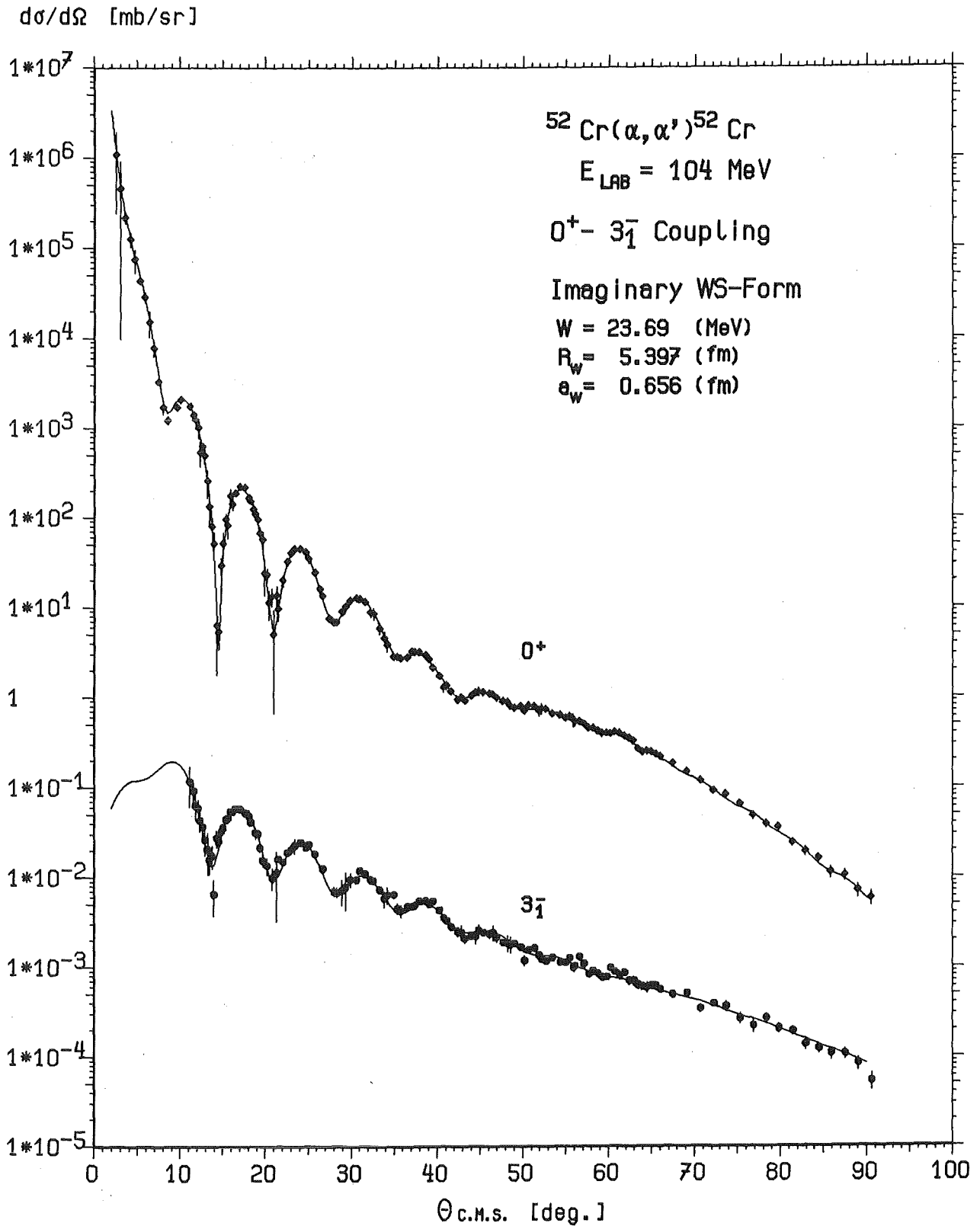


Fig. 2 Elastic and inelastic scattering of 104 MeV α -particles by ^{52}Cr : experimental cross sections and results of coupled channel calculations.

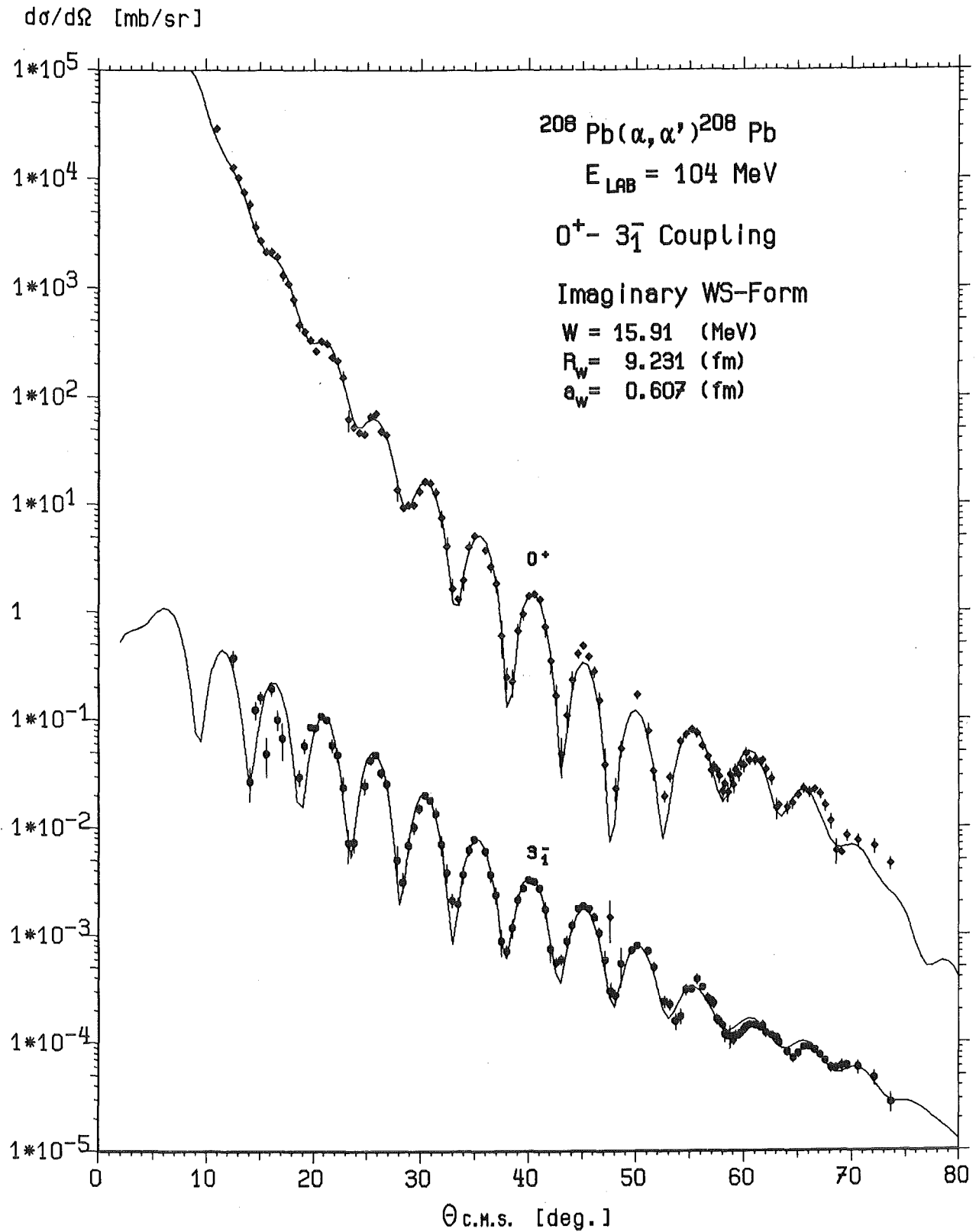


Fig. 3 Elastic and inelastic scattering of 104 MeV α -particles by ^{208}Pb : experimental cross sections and results of coupled channel calculations.

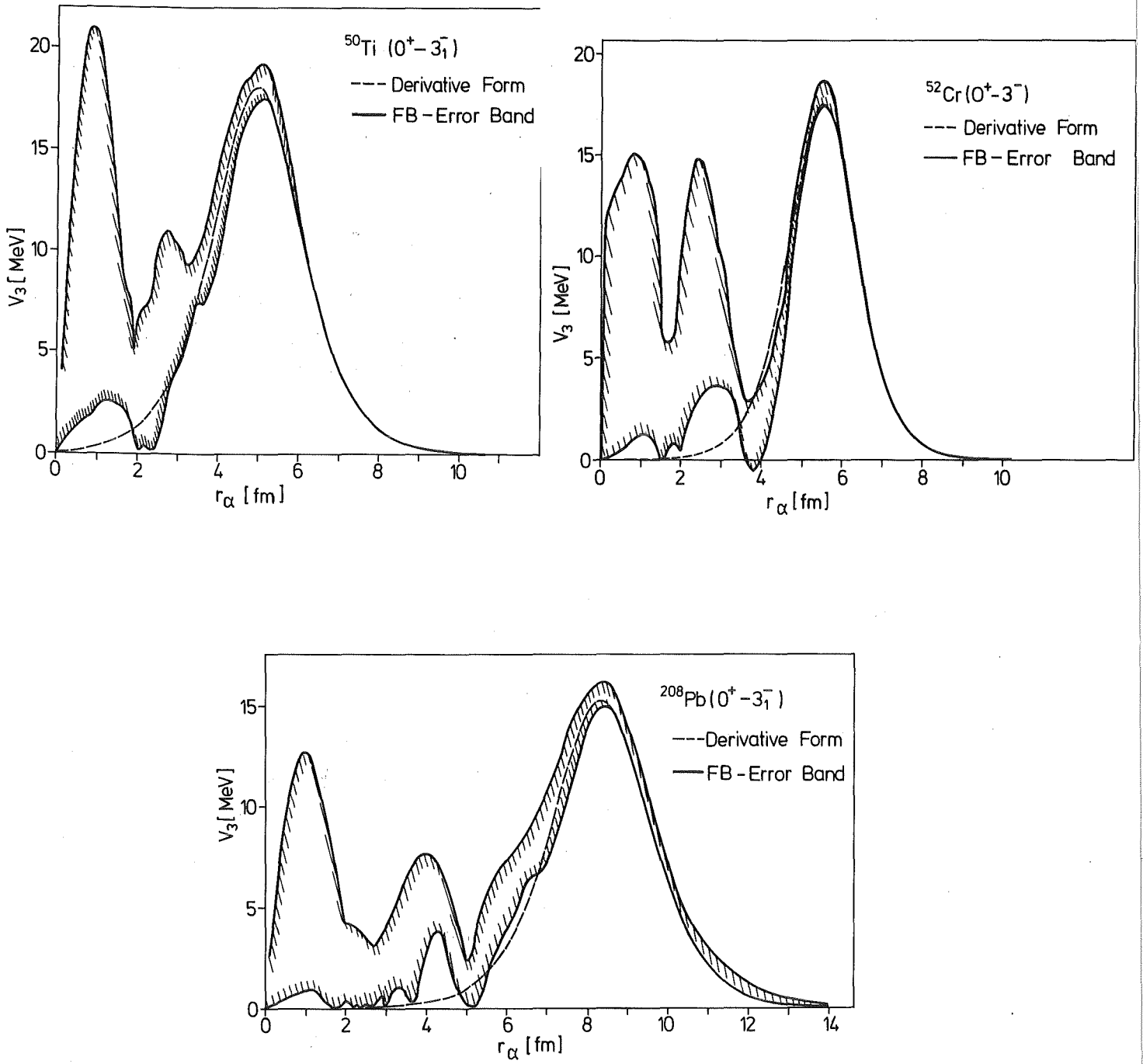


Fig. 4 Coupling potentials for the $0^+ - 3_1^-$ transitions in ^{50}Ti , ^{52}Cr and ^{208}Pb induced by 104 MeV α -particles.

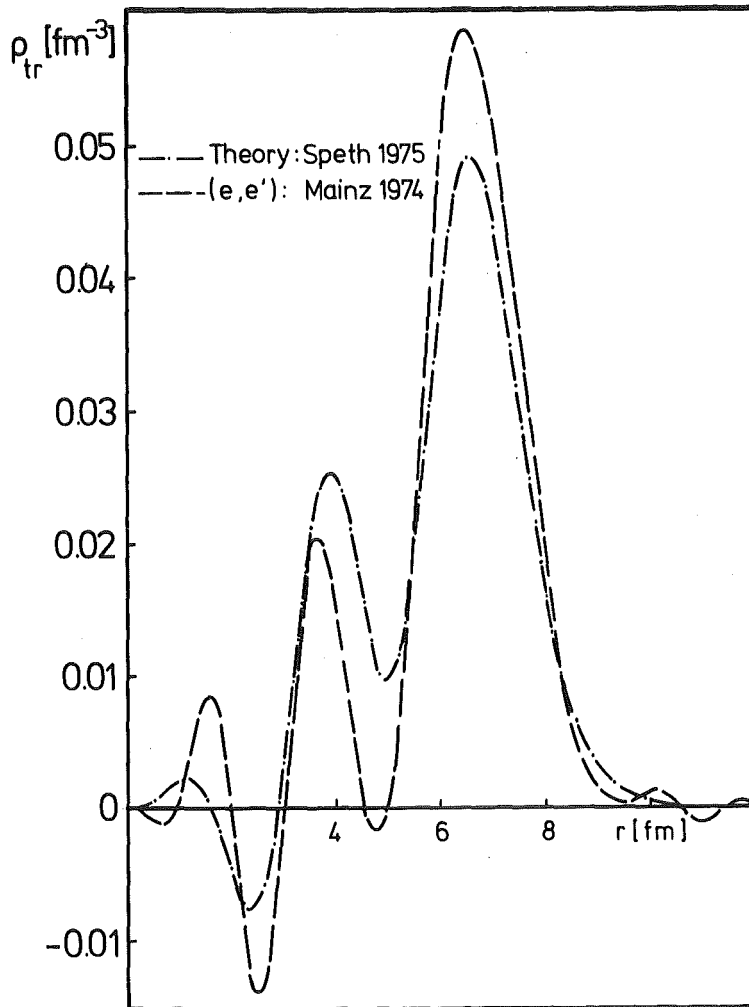


Fig. 5 Charge transition density of the $0^+ - 3_1^-$ transition in ^{208}Pb

3. ANALYSIS OF RADIAL MOMENTS

After the determination of the transition potentials we have the problem to relate them to the transition densities of the probed nucleus. Basically we assume that the real part of v_L has the structure of a folded potential, and applying simple mathematical relationships between the radial moments of folded distributions we deduce the transition moments of the nucleon distribution from the coupling potential via

$$\int v_L(r_\alpha) r_\alpha^{L+2} dr = \int \rho_L(r) r^{L+2} dr J_O(V_{\text{eff}}).$$

The α -particle-bound-nucleon interaction V_{eff} which need not be specified, enters (implicitly) by its volume integral $J_O(V_{\text{eff}})$. This quantity is related to the volume integrals of the monopole (diagonal) parts of the potential and of the density distribution, respectively

$$J_O(V_{\text{diag}}) = A J_O(V_{\text{eff}}). \quad (3.1)$$

With these relations we write the isoscalar transition rates⁺

$$B(IS, I_i \rightarrow I_f) = \frac{1}{2I_i+1} \left[\frac{Z}{A} \int \rho_L(r) r^{L+2} dr \right]^2 \quad (3.2)$$

directly as

$$B(IS, I_i \rightarrow I_f) = \frac{1}{2I_i+1} \left[\frac{Z}{J_O(V_{\text{diag}})} \int v_L(r_\alpha) r_\alpha^{L+2} dr_\alpha \right]^2. \quad (3.3)$$

The squared transition radius

$$R_{\text{tr}}^2(v_L) = \langle r^{L+2} \rangle / \langle r^L \rangle \quad (3.4)$$

of the potential v_L can be related to the corresponding quantity of the transition density ρ_L by

$$R_{\text{tr}}^2(v_L) = R_{\text{tr}}^2(\rho_L) + \frac{1}{3} (2L+3) \langle r^2 \rangle_{\text{eff}}. \quad (3.5)$$

For this the ms radius $\langle r^2 \rangle_{\text{eff}}$ of the effective interaction potential has to be known. Assuming that the real part of the α -particle nucleus optical potential can be understood as a folded potential, $\langle r^2 \rangle_{\text{eff}}$ is just the difference between the ms radii of the potential and of the underlying matter distribution.

⁺) The factor Z/A is usually introduced just for convenience when comparing with electromagnetic transitions.

Table 2 Volume integrals, rms and transition radii and transition rates for the $0^+ \rightarrow 3_1^+$ transitions in ^{50}Ti , ^{52}Cr and ^{208}Pb

Quantity	^{50}Ti	^{52}Cr	^{208}Pb	
$J_0(V_{\text{Diag}})/4A$ [MeV fm ³]	306 _{±6}	303 _{±4}	321 _{±7}	FB-analysis (elastic sc.)
$\langle r_{V_{\text{Diag}}}^2 \rangle^{1/2}$ [fm]	4.47 _{±0.12}	4.48 _{±0.09}	6.29 _{±0.18}	
$R_{\text{tr}}(\rho_3)$ [fm]	5.42 _{±0.22}	5.24 _{±0.16}	8.51 _{±0.32}	
G_3 (s.p.u.)	12.1 _{±0.5}	11.1 _{±0.3}	43.0 _{±1.3}	RMA of FB potentials
G_3 (s.p.u.)	11.7	9.8	37.6	RMA of WS-derivative
G_3 (s.p.u.)	-	6.1 _{±0.3}	38.4	electrom. ^{a,b}
G_3 (s.p.u.)	9.6	9.7	52.0	theoret. ^{c,d}

^a Endt (1979)

^b Rothaas et al. (1974)

^c Gillet et al. (1968)

^d Veje (1966)

Table 2 presents the results which are based on such an implicit folding model interpretation (RMA) of the real potentials found in the analysis of the experimental data. The values of the ms radius and the volume integrals of the diagonal part have been adopted from FB analyses of the elastic scattering. The value of $\langle r_{\text{eff}}^2 \rangle^{1/2} = 2.6$ fm can be deduced from previous results (Gils et al 1980) of elastic α -particle scattering on ^{40}Ca , for which the matter radius is believed to be known. There is an additional uncertainty. If the effective α -bound-nucleon interaction is density dependent and if the elastic and inelastic scattering probe different parts of the nucleus then $\langle r_{\text{eff}}^2 \rangle$ may differ slightly. The transition rates are represented by the enhancement factors $G_3 = B(IS, 0^+ \rightarrow 3_1^-) / B_{\text{s.p.}}$

(using the radius parameter $r_0 = 1.2$ fm in the definition of the single particle unit). In addition to the FB potentials the coupling potentials v_3 in the usual Saxon-Woods squared form (just of V_{trans} in Table 1) have been considered and results are given without any estimate of the uncertainties. It may be interesting to note that the evaluation procedure proposed by Bernstein (Bernstein 1969) results in $G_3 = 27.4$ s.p.u. for the $0^+ \rightarrow 3_1^-$ transition in ^{208}Pb . This discrepancy is just due to the underestimation by the factor $N = (\langle r^{L-1} \rangle_V / \langle r^{L-1} \rangle_m)^2$ as discussed by Wagner et al. (1982).

4. CONCLUDING REMARKS

The question of relative amount of neutron and proton strength in nuclear transitions is currently of considerable interest. Up to now only $0^+ - 2_1^+$ transitions, mostly in single-closed shell nuclei, have been seriously considered with this aspect, referring often to a vibrational model picture and discussing in terms of different nuclear deformations. The primary quantities, however, are the transition matrix elements which can be extracted in a less model dependent way. In this spirit, we applied a recently proposed method for analyzing inelastic α -particle scattering and present reliable values of isoscalar octupole transition rates in ^{50}Ti , ^{52}Cr and ^{208}Pb . In the case of ^{52}Cr and ^{208}Pb electromagnetic ($0^+ - 3_1^-$) transition rates are known and the comparison seems to reveal a significant difference in ^{52}Cr . While for the $0^+ - 2_1^+$ transition the proton transition strength appears to be stronger than the neutron transition strength (Rebel et al 1981, Lunke et al 1981), the pure isoscalar octupole transition rate is larger indicating some cancellation in the electromagnetic transition with isovector contribution (Veje 1966).

The International Bureau, Kernforschungszentrum Karlsruhe, and the Central Institute of Physics, Bucharest, have supported the collaboration. We are grateful to Prof. Dr. G. Schatz for his interest in these studies and acknowledge valuable discussions with Prof. Dr. G.J. Wagner.

REFERENCES

- Amado R D, Lenz F, McNeil J A and Sparrow D A
1980 Phys. Rev. C22, 204.
- Bernstein A M 1969 Advances in Nuclear Physics
Vol. 3, ed. M. Baranger and E. Vogt
(New York: Plenum Press) p 325
- Bernstein A M, Brown V R and Madsen V A
1981 Phys. Lett. 103B 255
- Brown B A and Wildenthal B M
1980 Phys Rev C21 2107
- Brown V R and Madsen V A 1975 Phys. Rev. C11 1298
Brown V R and Madsen V A 1978 Phys. Rev. C17 1943
- Endt P M 1979 Atomic and Nucl. Data Tables
Vol 23/6 547
- Friedman E, Gils H J, Rebel H and Pesl R 1981
Nucl. Phys. A363 137
- Gillet V, Giraud B, Picard J and Rho M
1968, Phys. Lett 27B 483
- Gils H J, Friedman E, Rebel H, Buschmann J, Zagromski S,
Klewe-Nebenius H, Neumann B, Pesl R and Bechtold G,
1980, Phys. Rev. C21 1239
- Lunke C, Egger J P, Goetz F, Gretillat P, Schwarz E,
Perrin C, Preedom B M and Mischkew R E 1981, J. Phys.
G: Nucl. Phys. 7 895
- Pesl R, Gils H J, Rebel H, Buschmann J, Klewe-Nebenius H,
and Zagromski S, 1982, KfK 3378 and to be published

Rebel H 1976, Z. Phys. A277 35

Rebel H, Pesl R, Gils H J and Friedman E
1981 Nucl. Phys. A368 61

Rothaas H, Friedrich J, Merle K and Dreher B 1974
Phys. Lett 51B 23

Schweimer W and Raynal J 1973, unpublished results and
private communications

Speth J 1976, private communication

Theis W and Werner E 1973, Phys. Lett. 44 B 481

Veje C J 1966 Mat. Fys. Medd. Dan. Vid. Selsk
35 No. 1

Wagner G J, Grabmayr P and Schmidt H R 1982
Phys. Lett. (in press)